

Assembly and evaluation of a pyroelectric detector bonded to vertically aligned multiwalled carbon nanotubes over thin silicon

E. Theocharous,^{1,*} S. P. Theocharous,² and J. H. Lehman³

¹National Physical Laboratory, Hampton Road, Teddington TW11 0LW, UK

²Physics Department, Imperial College, London SW7 2BZ, UK

³National Institute of Standards and Technology, Boulder, Colorado 80305, USA

*Corresponding author: e.theo@npl.co.uk

Received 4 September 2013; revised 1 October 2013; accepted 1 October 2013;
posted 28 October 2013 (Doc. ID 196977); published 15 November 2013

A novel pyroelectric detector consisting of a vertically aligned nanotube array on thin silicon (VANTA/Si) bonded to a 60 μm thick crystal of LiTaO_3 has been fabricated. The performance of the VANTA/Si-coated pyroelectric detector was evaluated using National Physical Laboratory's (NPL's) detector-characterization facilities. The relative spectral responsivity of the detector was found to be spectrally flat in the 0.8–24 μm wavelength range, in agreement with directional-hemispherical reflectance measurements of witness samples of the VANTA. The spatial uniformity of response of the test detector exhibited good uniformity, although the nonuniformity increased with increasing modulation frequency. The nonuniformity may be assigned either to the dimensions of the VANTA or the continuity of the bond between the VANTA/Si coating and the pyroelectric crystal substrate. The test detector exhibited a small superlinear response, which is similar to that of pyroelectric detectors coated with good quality gold-black coatings.

OCIS codes: (040.3060) Infrared; (040.6808) Thermal (uncooled) IR detectors, arrays and imaging; (120.1880) Detection; (230.0040) Detectors.

<http://dx.doi.org/10.1364/AO.52.008054>

1. Introduction

The choice of the absorptive coating is very important in determining the performance of a thermal detector [1]. The addition of a black coating to the active area of the thermal detector increases the fraction of incident radiation that is absorbed and converted into heat, but also increases the heat capacity and hence reduces the temperature rise of the detector-coating composite. It is important that black coatings have high absorptivity, and also intrinsically low thermal capacity. These requirements are all satisfied by vertically aligned nanotube array (VANTA) coatings, which have been shown to combine very high absorptivity values [2–5] and very low thermal capacities. Absorptive coatings applied to thermal detectors should also have high thermal conductivities. This condition is also satisfied by

VANTA coatings, which have been shown to have high thermal conductivity axially as well as transverse to the nanotube forest [6,7].

Despite the potential advantages of VANTA coatings over other black coatings [8], they have yet to be widely applied as absorptive coatings for thermal detectors because VANTA coatings have only been reliably grown on high-mass super alloys and on thermally stable materials such as silicon [3,4]. The main obstacle to putting a VANTA coating on a pyroelectric transducer is that VANTA coatings are grown at substrate temperatures of about 750°C in a reducing atmosphere. The growth temperature is well above the Curie point of pyroelectric materials such as LiTaO_3 (~660°C) and the growth conditions modify the dielectric properties of the crystal by diffusion of oxygen from the surface.

This paper describes the evaluation of a pyroelectric detector having a novel composite VANTA-on-silicon absorber. The thin silicon substrate on which the VANTA coating was grown was bonded to a 60 μm thick LiTaO_3 pyroelectric crystal, which acts as the detector transducer. This paper describes the fabrication of the new detector and the evaluation of its radiometric characteristics.

2. Method

A. Fabrication of the VANTA/Si-Coated Pyroelectric Detector

A variety of methods have been used to apply carbon nanotubes to a thermal detector, e.g., bulk nanotubes sprayed on pyroelectric materials [9], a freestanding forest transferred from a silicon substrate to a pyroelectric or thermopile detector [10], direct growth onto a pyroelectric by means of chemical vapor deposition (CVD) [11], and hot-wire CVD [12]. These approaches all come with compromises with respect to cost, detector performance, and fabrication yield. In the present work, rather than removing the nanotube forest from a silicon growth substrate and transferring it to the pyroelectric substrate, we leave the nanotubes on the silicon substrate. In order to minimize the heat capacity, we grew the nanotube forest on relatively thin silicon (we refer to this subassembly as VANTA/Si) and bonded the VANTA/Si directly to the pyroelectric detector electrode.

Figure 1 shows a flow chart that summarizes the process that was used to fabricate the pyroelectric detector with the VANTA/Si coating. The nanotubes were grown by CVD in a 15 cm quartz tube furnace. The 10 μm thick silicon wafer, which was approximately 8 mm \times 8 mm, was coated with 5 nm of Al_2O_3 and that was over-coated by 1.1 nm thick coating of Fe-based catalyst. The silicon substrate was introduced into the furnace chamber and ramped to the set point temperature of 780°C while flowing Ar [3250 standard cubic centimeters per minute (sccm)] and H_2 (580 sccm) through the tube. The forest growth was carried out at atmospheric

pressure while maintaining the same temperature by adding C_2H_4 gas (300 sccm) to the flow.

The pyroelectric detector element was constructed from a 60 μm thick, 12 mm diameter, lithium tantalate (LiTaO_3) crystal. Circular electrodes, 10 mm in diameter, were deposited on each face of the crystal which consisted of 50 nm of gold on top of 25 nm of chromium on the back face and 25 nm of chromium on the front face (the face to which the VANTA/Si was attached).

The VANTA/Si was attached to the front electrode with silver-filled, two part electrically conducting epoxy. The epoxy was applied in a thin layer, less than 2 μm thick, with a nylon swab. The VANTA/Si was placed on the epoxy layer and the assembly of VANTA/Si/ LiTaO_3 was placed in a bell jar that was evacuated for 30 min.

The composite VANTA/Si/ LiTaO_3 stack was assembled into a detector package such that the front electrode was the electrical “earth ground” while the back electrode was the “signal electrode.” Electrical connection was then made to a separate transimpedance amplifier. The front face of the detector was defined by a 3 mm aperture placed in front of the area defined by the VANTA/Si coating.

B. Method of Evaluating the Performance of the Test Detector

The relative spectral responsivity of the VANTA/Si detector was measured in the 0.8 to 24 μm wavelength range on the National Physical Laboratory (NPL) infrared spectral responsivity characterization facility. This measurement involved the direct comparison of the spectral responsivity of the test detector with the responsivity of an NPL spectral responsivity transfer standard detector [13]. This allowed the spectral flatness of the absorptivity of the VANTA coating to be determined and compared with absolute absorptivity measurements made on witness samples of the VANTA coatings [14]. All relative spectral responsivity measurements were made using radiation modulated at 80 Hz.

The absolute spectral responsivity of the test detector was measured by direct comparison to the spectral responsivity of an InGaAs transfer standard detector at 1.5 μm on the NPL infrared spectral responsivity facility using a 2 mm diameter spot centered on the active area of the test detector. The calibration of the absolute spectral responsivity of the InGaAs transfer standard detector was traceable to the NPL cryogenic radiometer [15].

The spatial uniformity of response of a detector defines the ability of a detector to give a constant output if the same radiant flux is incident on different parts of the detector active area. The spatial uniformity of response of the VANTA/Si-coated test detector was measured using the NPL spatial uniformity of response measurement facility [16]. A 0.16 mm diameter light spot was scanned over the active area of the test detector. Measurements were repeated at three different modulation frequencies in order

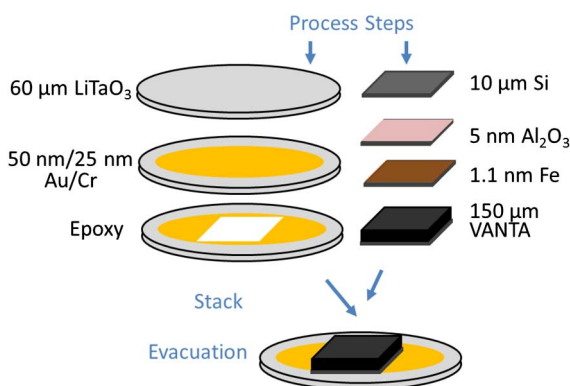


Fig. 1. Flow chart summarizing the process that was used to fabricate the pyroelectric detector with the VANTA-on-silicon coating.

to determine the dependence on the modulation frequency. The same facility was also used to map the spatial distribution of the phase delay introduced by the presence of the VANTA coating. The phase delay provided information on the spatial uniformity of the thermal diffusivity of the VANTA coating [17].

The linearity of response of a detector describes how the responsivity of the detector changes as a function of the incident optical radiant power. The linearity of response of the VANTA-coated detector was measured on the NPL linearity of response measurement facility [16], which uses the flux superposition method. This measurement also provides information on the thermal diffusivity and thermal conductivity of the VANTA coating [17]. Finally, the response of the test detector to incident radiant power modulated at a range of frequencies was measured and was compared with the corresponding measurement of an uncoated LiTaO₃ pyroelectric detector of identical thickness.

3. Results and Discussion

A. Spectral Responsivity

The test detector offers superior SNR characteristics compared to previous VANTA-coated pyroelectric detectors [17], so the spectral responsivity measurements were extended to 24 μm . Figure 2 shows the relative spectral responsivity of the VANTA/Si-coated pyroelectric detector in the 0.8–24 μm wavelength range, normalized at a wavelength of 1 μm . The error bars shown in Fig. 2 represent the standard uncertainty of the measurements [13]. Figure 2 shows that the spectral responsivity of the test detector is spectrally flat (within the uncertainty of the measurements) over the entire wavelength range of measurements. Since the absorption characteristics of the VANTA/Si coating govern the relative spectral responsivity characteristics of the test detector [1], it can be concluded that the VANTA coating deposited on the test detector has a spectrally flat absorbance over the 0.8–24 μm wavelength range. This, in combination with absolute directional-hemispherical reflectance measurements made at NPL on witness VANTA samples [5], indicate that the VANTA coating deposited on the test detector

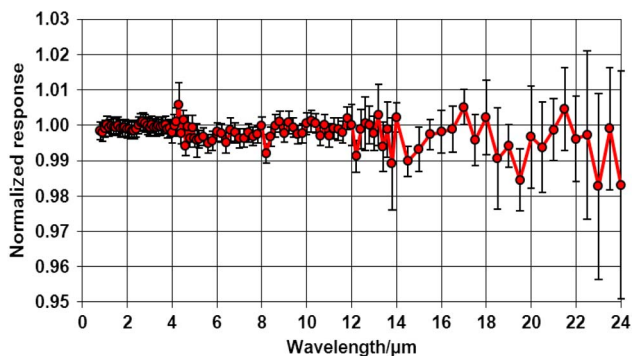


Fig. 2. Relative spectral responsivity of the VANTA-on-Si pyroelectric detector, normalized at 1 μm .

combines high absorptivity with spectral flatness. This confirms the attraction of VANTA coatings for a number of applications, including as coatings for thermal detectors in the infrared.

The DC equivalent radiant power responsivity of the VANTA/Si test detector operated in photocurrent mode for a modulation frequency of 80 Hz was measured to be $5.9 \times 10^{-7} \text{ AW}^{-1}$ at 1.5 μm . This is 30% higher than the corresponding absolute spectral responsivity of an uncoated LiTaO₃ pyroelectric detector of similar crystal thickness (60 μm thick). However, in radiometry, the real benefit of the black VANTA/Si coating is not provided by the 30% higher absolute responsivity but lies in the fact that the presence of the black coating gives the pyroelectric detector a spectrally flat response [13].

B. Spatial Uniformity of Response Evaluation

Figure 3 shows the spatial uniformity of response of the VANTA/Si-coated detector recorded using chopped radiation at 80 Hz modulation frequency. Figures 4 and 5 show the corresponding spatial uniformity plots measured using 20 and 8 Hz modulation frequencies, respectively. Figures 3–5 indicate that the spatial uniformity of response improves as the modulation frequency of the incident radiant power decreases. Whereas the peak to peak spatial nonuniformity of this detector only improves from 4% to 3% as the modulation frequency decreased from 80–8 Hz, the fine structure that was present in the spatial uniformity of response at 80 Hz is absent at 8 Hz. The spatial uniformity of response of LiTaO₃ pyroelectric detectors coated with sprayed multi wall carbon nanotube (MWCNT) coatings was also observed to deteriorate with increasing modulation frequency but the change was much higher, increasing from 18% at

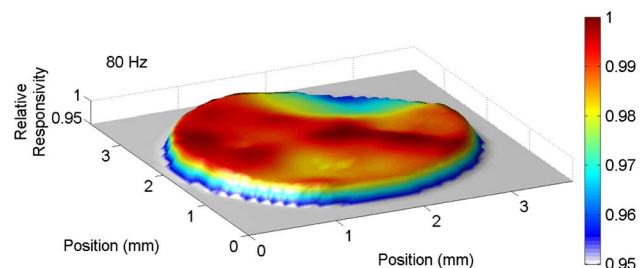


Fig. 3. Spatial uniformity of response of the test detector at 80 Hz using a 160 μm diameter spot.

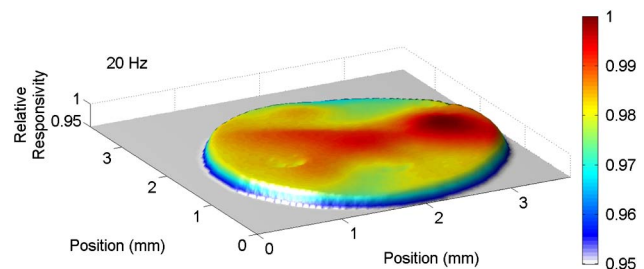


Fig. 4. Spatial uniformity of response of the test detector at 20 Hz using a 160 μm diameter spot.

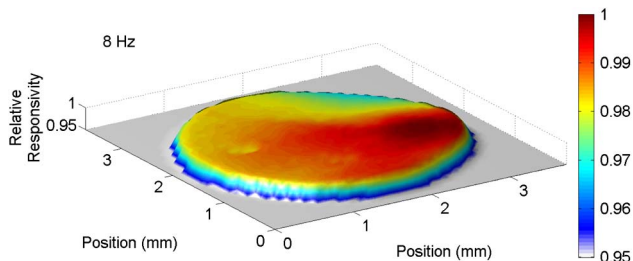


Fig. 5. Spatial uniformity of response of the test detector at 8 Hz using a 160 μm diameter spot.

8 Hz to over 60% at 80 Hz [18]. Furthermore, there was considerably more fine structure in the spatial uniformity of response of the LiTaO_3 pyroelectric detectors coated with sprayed MWCNT coatings [18]. However, what hinders the adoption of sprayed MWCNT coatings in infrared radiation metrology is not their poorer spatial uniformity of response but the lower absorbance associated with sprayed MWCNT coatings (it can be as low as 90% in the infrared), combined with spectral variations in their absorbance. In particular, the absorbance of sprayed MWCNT coatings decreases with increasing wavelength, in contrast with VANTA coatings, which have been applied to LiTaO_3 pyroelectric detectors and have near unity absorbance values for wavelengths beyond 20 μm [5].

C. Linearity of Response

Figure 6 shows the linearity factor [19] of the VANTA-coated test detector as a function of the lock-in amplifier output rectifying the detector output. Measurements were repeated at two different modulation frequencies, 8 and 80 Hz. A 2 mm diameter spot was illuminating the geometric center of the test detector in all linearity measurements reported. Figure 6 shows that there is good overlap of the measurements corresponding to the two modulation frequencies, indicating that the linearity characteristics of the test detector are not dependent on the modulation frequency in the 8–80 Hz range. The error bars represent the standard deviation of

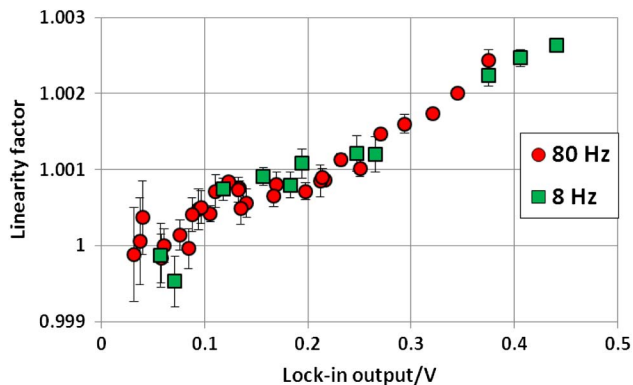


Fig. 6. Plot of the linearity factor of the VANTA-coated test detector as a function of the lock-in amplifier output when a 2 mm diameter spot was incident on the active area of the test detector. Measurements at 8 and 80 Hz modulation frequencies are shown.

at least eight repeat measurements. The linearity factor of the test detector exhibits a superlinear response, i.e., the linearity factor increases with increasing detector output. This behavior was also observed in other LiTaO_3 pyroelectric detectors [19], and arises due to the positive temperature coefficient of response of LiTaO_3 pyroelectric crystals. The superlinear response indicates that the thermal diffusivity of the VANTA/Si coating is high. LiTaO_3 pyroelectric detectors coated with black coatings of low thermal diffusivity were found to exhibit a sub-linear response [19].

D. Dependence of the Output on the Modulation Frequency

Figure 7 shows the normalized output of the VANTA-coated pyroelectric detector at different modulation frequencies in the 4–120 Hz range, normalized to a modulation frequency of 4 Hz. Also shown in Fig. 7 is the corresponding plot for an uncoated LiTaO_3 pyroelectric detector of the same thickness. The fact that the response does not change strongly with modulation frequency indicates that the absorptive coating has high thermal diffusivity. Figure 7 also shows the plot corresponding to another LiTaO_3 pyroelectric detector coated with a VANTA coating but bonded on the pyroelectric crystal using alumina paste [17]. The plot corresponding to the detector with the VANTA coating bonded with alumina paste is very different from the other two, providing further confirmation that the thermal diffusivity of this coating (i.e., the coating bonded with alumina paste) is poor compared to the VANTA/Si-coated pyroelectric detector and, of course, the uncoated detector.

Figure 8 shows the normalized output of a 60 μm thick LiTaO_3 pyroelectric detector coated with a sprayed MWCNT coating [18] at different modulation frequencies in the 4–120 Hz range, normalized to a modulation frequency of 4 Hz, for comparison. Figure 8 shows that the response of the detector coated with the sprayed MWCNT coating at 120 Hz decreased to 19% of its value at 4 Hz whereas the response of the uncoated detector at 120 Hz decreased to 67% of its value at 4 Hz. This indicates

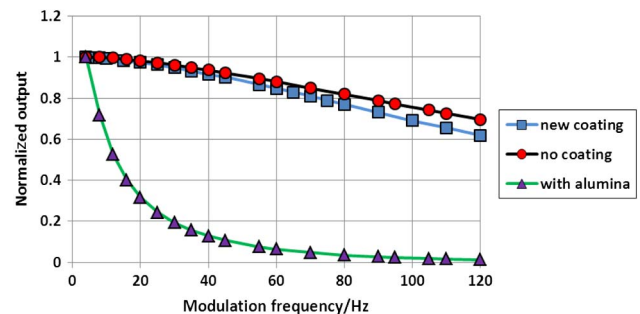


Fig. 7. Normalized output of the VANTA-on-Si-coated pyroelectric detector as a function of modulation frequency. Also shown are the corresponding plots for an uncoated pyroelectric detector and a pyroelectric detector coated with a VANTA coating, but bonded to the pyroelectric crystal using alumina paste.

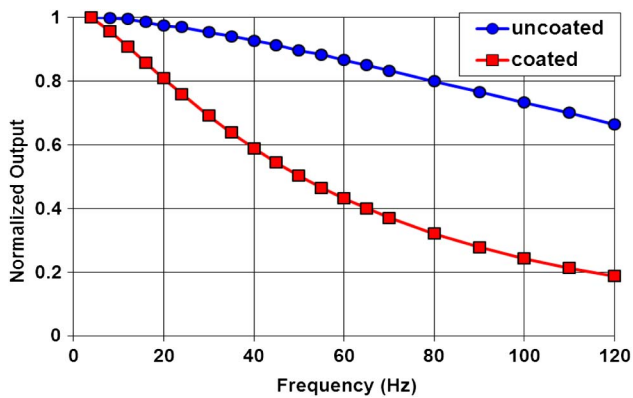


Fig. 8. Normalized output of a pyroelectric detector coated with a sprayed MWCNT coating, as a function of modulation frequency. Also shown is the corresponding plot for the uncoated pyroelectric detector, for comparison.

that the thermal diffusivity of the sprayed MWCNT coating is lower than that of the VANTA-on-silicon coating. The thermal diffusivity of the sprayed MWCNT coating can be improved by decreasing its thickness but that is associated with a severe decrease of its absorbance, particularly at longer wavelengths.

E. Phase Mapping

The delay in the phase of the output electrical signal from the VANTA-coated pyroelectric detector relative to the phase of the incident modulated beam was mapped at every point on the active area of the test detector using a modified version of the NPL spatial uniformity of response measurement facility. The beam was modulated with square wave modulation before it was incident on the detector. Absorption of the modulated beam by the black coating produced heat waves which propagate through the VANTA/Si coating, before they reach the pyroelectric crystal where they are converted into electrical signals. The thermal diffusivity of the coating is a unique function of the phase difference measured and the thickness of the coating [20]. The phase difference was mapped by scanning the incident spot on the front face of the test detector. Figure 9 shows the spatial distribution of the phase difference

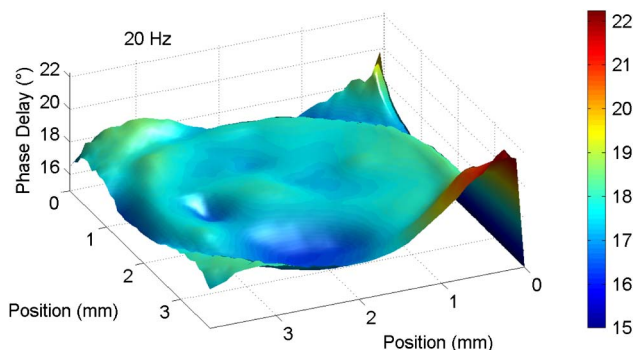


Fig. 9. Phase delay measured with a 20 Hz modulation frequency, mapped using a 160 μm diameter spot.

between the output electrical signal and the modulated beam incident on VANTA/Si-coated test detector, measured for a modulation frequency of 20 Hz. Figure 8 shows that the phase difference varied by only 2° over the entire active area of the test detector. The corresponding spatial variations of the phase delay that were observed for the VANTA coating bonded with alumina paste were about 20° over the active area of the detector [17], indicating that the spatial uniformity of the thermal diffusivity of the VANTA-on-Si black coating is far superior compared to the spatial uniformity of the thermal diffusivity of the VANTA coating attached with alumina paste.

4. Summary and Conclusions

A novel method was used to apply a VANTA coating onto a 60 μm thick LiTaO_3 pyroelectric detector. The black coating was grown on a silicon substrate and the VANTA coating-silicon substrate combination was bonded on the pyroelectric crystal substrate. The performance of the VANTA/Si-coated pyroelectric detector was evaluated using NPL's detector characterization facilities. The relative spectral responsivity of the VANTA/Si-coated detector was shown to be spectrally flat in the 0.8–24 μm wavelength range, in agreement with directional-hemispherical reflectance measurements of witness samples of the VANTA coatings. The absolute spectral responsivity of the test detector was 30% higher than that of an uncoated 3 mm diameter LiTaO_3 pyroelectric detector, demonstrating one of the benefits of the VANTA coating. The spatial uniformity of response of the test detector exhibited good uniformity, although the nonuniformity increased with modulation frequency. The nonuniformity may be assigned either to variations in the thickness of the VANTA/Si composite or to the uniformity of the bond to the pyroelectric crystal substrate. The test detector exhibited a small superlinear response, and this behavior is in agreement with that of other pyroelectric detectors coated with high diffusivity black coatings. This observation confirms that the thermal conductivity of the VANTA/Si coating is high and confirms that the thermal conductivity of the component MWCNTs which make up the VANTA coating is high along their lengths.

E. T. acknowledges support from the National Measurement Office of the UK Department of Business, Innovation and Skills.

References

1. W. R. Blevin and J. Geist, "Influence of black coatings on pyroelectric detectors," *Appl. Opt.* **13**, 1171–1178 (1974).
2. Z. P. Yang, L. Ci, J. A. Bur, S. Y. Lin, and P. M. Ajayan, "Experimental observation of extremely dark material made by a low-density nanotube array," *Nano Lett.* **8**, 446–451 (2008).
3. K. Mizuno, J. Ishii, H. Kishida, Y. Hayamizu, S. Yasuda, D. N. Futaba, M. Yumura, and K. Hata, "A black body absorber from vertically aligned single-walled carbon nanotubes," *Proc. Natl. Acad. Sci. USA* **106**, 6044–6047 (2009).

4. M. A. Quijada, J. G. Hagopian, S. Getty, R. E. Kinzer, and E. J. Wollack, "Hemispherical reflectance and emittance properties of carbon nanotube coatings at infrared wavelengths," *Proc. SPIE* **8150**, 815002 (2001).
5. C. J. Chunnillall, J. H. Lehman, E. Theocharous, and A. Sanders, "Infrared hemispherical reflectance of carbon nanotube mats and arrays in the 5–50 μm wavelength region," *Carbon* **50**, 5348–5350 (2012).
6. S. Berber, Y. Kwon, and D. Tomanek, "Unusually high thermal conductivity of carbon nanotubes," *Phys. Rev. Lett.* **84**, 4613–4616 (2000).
7. A. Okamoto, I. Gunjishima, T. Inoue, M. Akoshima, H. Miyagawa, T. Nakano, T. Baba, M. Tanemura, and G. Oomi, "Thermal and electrical conduction properties of vertically aligned carbon nanotubes produced by water-assisted chemical vapor deposition," *Carbon* **49**, 294–298 (2011).
8. J. Lehman, E. Theocharous, G. Eppeldauer, and C. Pannel, "Gold-black coatings for freestanding pyroelectric detectors," *Meas. Sci. Technol.* **14**, 916–922 (2003).
9. J. H. Lehman, C. Engtrakul, T. Gennett, and A. C. Dillon, "Single-wall carbon nanotube coating on a pyroelectric detector," *Appl. Opt.* **44**, 483–488 (2005).
10. J. H. Lehman, B. Lee, and E. N. Grossman, "Far infrared thermal detectors for laser radiometry using a carbon nanotube array," *Appl. Opt.* **50**, 4099–4104 (2011).
11. J. Lehman, A. Sanders, L. Hanssen, B. Wilthan, J. Zeng, and C. Jensen, "Very black infrared detector from vertically aligned carbon nanotubes and electric-field poling of lithium tantalate," *Nano Lett.* **10**, 3261–3266 (2010).
12. J. H. Lehman, R. Deshpande, P. Rice, and A. C. Dillon, "Carbon multi-walled nanotubes grown by HWCVD on a pyroelectric detector," *Infrared Phys. Technol.* **47**, 246–250 (2006).
13. E. Theocharous, "The establishment of the NPL infrared relative spectral response scale using cavity pyroelectric detectors," *Metrologia* **43**, S115–S119 (2006).
14. C. J. Chunnillall and E. Theocharous, "Infrared hemispherical reflectance measurements in the 2.5 μm to 50 μm wavelength region using an FT spectrometer," *Metrologia* **49**, S73–S80 (2012).
15. N. P. Fox, P. R. Haycocks, J. E. Martin, and I. Ul-Haq, "A mechanically cooled portable cryogenic radiometer," *Metrologia* **32**, 581–584 (1995-96).
16. E. Theocharous, F. J. J. Clarke, L. J. Rodgers, and N. P. Fox, "Latest techniques at NPL for the characterization of infrared detectors and materials," *Proc. SPIE* **5209**, 228–239 (2003).
17. S. P. Theocharous, E. Theocharous, and J. H. Lehman, "The evaluation of the performance of two pyroelectric detectors with vertically aligned multi-walled carbon nanotube coatings," *Infrared Phys. Technol.* **55**, 299–305 (2012).
18. E. Theocharous and J. Lehman, "The evaluation of a pyroelectric detector with a sprayed carbon multi-wall nanotube black coating in the infrared," *Infrared Phys. Technol.* **54**, 34–38 (2011).
19. E. Theocharous, "Absolute linearity measurements on LiTaO_3 pyroelectric detectors," *Appl. Opt.* **47**, 3397–3405 (2008).
20. S. B. Lang, E. Ringgaard, S. Muensit, X. Wu, J. C. Lashley, and Y. Wong, "Thermal diffusivity by laser intensity modulation method (LIMM-TD)," *IEEE Trans. Ultrason. Ferroelectr. Freq. Control* **54**, 2608–2616 (2007).